Acknowledgements We thank M. G. Farquhar and R. V. Stan for critically evaluating Weibel–Palade bodies; D. Chambers for conducting FACS analysis; J. Simon for help in constructing figures; L. Moore, B. Miller, A. Hyunh and S. Thuret for technical assistance; J. D. Esko's laboratory for advice; V. A. Sciorra and M. L. Gage for critical reading of the manuscript. This work was supported by the National Institutes of Health (National Institute on Aging) and the Lookout Fund. A.E.W. is a Damon Runyon fellow supported by The Damon Runyon Cancer Research Foundation. K.N. was supported by a JSPS Postdoctoral Fellowship for Research Abroad. F.H.G. is supported by the Vi and John Adler Chair.

Competing interests statement The authors declare competing financial interests: details accompany the paper on **www.nature.com/nature**.

Correspondence and requests for materials should be addressed to F.H.G. (gage@salk.edu).

The homeotic protein AGAMOUS controls microsporogenesis by regulation of *SPOROCYTELESS*

Toshiro Ito[1], Frank Wellmer[1], Hao Yu[1,2], Pradeep Das[1], Natsuko Ito[1], Márcio Alves-Ferreira[1,3], José Luis Riechmann[1] & Elliot M. Meyerowitz[1]

[1]*Division of Biology 156-29, California Institute of Technology, 1200 E. California Blvd, Pasadena, California 91125, USA*
[2]*Department of Biological Sciences, Faculty of Science, National University of Singapore, 10 Science Drive 4, 117543, Singapore*
[3]*Department of Genetics, Federal University of Rio de Janeiro, Av. Pau Brazil 211 A2-76, 21941-590, Rio de Janeiro, Brazil*

The *Arabidopsis* homeotic gene *AGAMOUS* (*AG*) is necessary for the specification of reproductive organs (stamens and carpels) during the early steps of flower development[1–3]. *AG* encodes a transcription factor of the MADS-box family that is expressed in stamen and carpel primordia. At later stages of development, *AG* is expressed in distinct regions of the reproductive organs[2–5]. This suggests that AG might function during the maturation of stamens and carpels, as well as in their early development. However, the developmental processes that AG might control during organogenesis and the genes that are regulated by this factor are largely unknown. Here we show that microsporogenesis, the process leading to pollen formation, is induced by AG through activation of the *SPOROCYTELESS* gene (*SPL*, also known as *NOZZLE,NZZ*), a regulator of sporogenesis[6,7]. Furthermore, we demonstrate that SPL can induce microsporogenesis in the absence of AG function, suggesting that AG controls a specific process during organogenesis by activating another regulator that performs a subset of its functions.

AG triggers reproductive organ development[8,9], a process which presumably involves temporally and spatially specific expression of a large number of genes[10]. However, only a few putative target genes of AG are currently known[11–13]. One of these genes is the MADS-box gene *SHATTERPROOF2* which shares partially redundant functions with AG in addition to its function in fruit dehiscence[12,14,15]. No other putative target genes have been identified that may function downstream of AG during floral organ formation.

To analyse the processes downstream of AG, we produced a strain with inducible AG activity. This strain is homozygous for the *ag-1*-null mutation and transgenic for *35S::AG–GR*, a constitutive promoter-driven *AG* gene with a carboxy-terminal fusion to the steroid-binding domain of the rat glucocorticoid receptor[16,17]. Plants of this genotype make *ag-1* mutant flowers, with indefinite numbers of successive whorls of sepal–petal–petal (Fig. 1a). Continuous treatment with the steroid hormone dexamethasone (DEX)—which leads to a translocation of the fusion protein from the cytoplasm to the nucleus—resulted in flowers with functional stamens and carpels, which resemble the flowers of *35S::AG* plants[8] (Fig. 1b). Thus, the AG–GR fusion protein can perform the function of AG. In contrast, a single DEX treatment resulted in only a partial phenotypic rescue; flowers bore petals with stamenoid structures (Fig. 1c). Most of the petals produced in whorl 3 of these flowers had locules (pollen sacs) at the lateral edges containing normal-looking pollen grains (Fig. 1d–f). These results show that a single DEX treatment is not enough to produce normal stamens, but is sufficient to induce microsporogenesis.

The strain with inducible AG activity was used in a gene expression profiling experiment performed with a complementary DNA microarray[10]. Several AG-responsive genes were identified, one of which was *SPL* (see Supplementary Fig. S1). *SPL* encodes a putative transcription factor, and has been implicated in ovule pattern formation and early microsporogenesis[6,7,18]. In *spl* mutants, the differentiation of primary sporogenous cells as well as anther wall formation are blocked. This results in mutant anthers that lack pollen grains[6,7]. The induction of *SPL* by AG activity was confirmed by semi-quantitative polymerase chain reaction with reverse transcription (RT–PCR), as well as real-time PCR (Fig. 2a; see also Supplementary Fig. S2). AG-dependent *SPL* upregulation was detected at the 4 hour time-point, and the signal became stronger at 8 h, remaining relatively stable afterwards. We next tested whether AG activates *SPL* in the presence of 10 μM cycloheximide, an efficient inhibitor of protein synthesis[17,19]. Cycloheximide did not block the induction of *SPL* by AG, suggesting that this induction might be direct (Fig. 2a).

To examine whether there are putative binding sites of AG in the *SPL* promoter, the *SPL* genomic region was examined for the 16-base pair consensus binding sequence of AG[20,21], which contains the 10-bp 'CArG-box core' ($5'$-CCNN(A/T)$_4$GG-$3'$). In the $3'$ region of the gene (897 bp downstream from the stop codon), one site was identified that contains a single mismatch from the consensus sequence of the CArG box (Fig. 2b). An electrophoretic

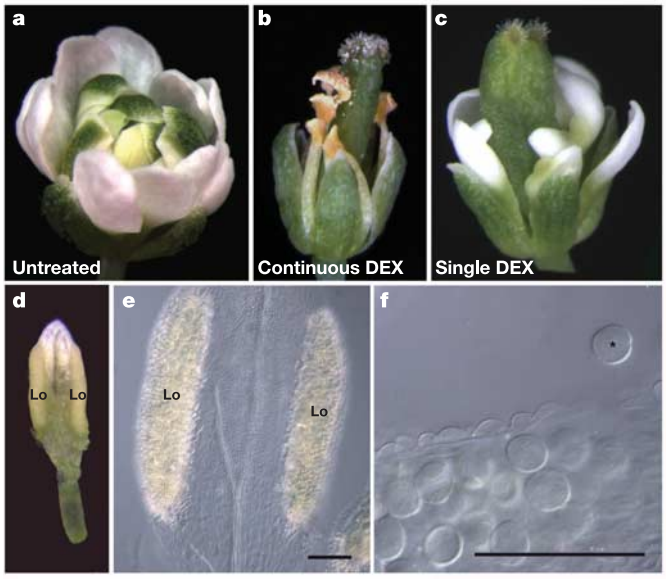

Figure 1 Activation of AG–GR rescues the *ag-1* mutant phenotype. **a**–**c**, Flowers from *ag-1 35S::AG–GR* plants untreated (**a**), or after continuous (**b**), or a single (**c**) DEX treatment. Treatments were initiated 12 days before imaging. Four DEX treatments at 0.5-day intervals, or three treatments at 2-day intervals, were sufficient to fully rescue the mutant phenotypes (data not shown). **d**, Petal with loculed structures produced in whorl 3 of the flower shown in **c**. **e**, **f**, Close-up of a loculed petal after clearing. Morphologically normal pollen grains (**f**) were produced in the locules (**e**). Asterisk indicates a pollen grain released by manually breaking a locule. Lo, locules. Scale bars, 100 μm.

mobility shift assay using a synthetic DNA probe showed that recombinant AG protein binds to this sequence *in vitro* (Fig. 2c). The binding was increased when the single mismatch of the wild-type sequence was altered to produce the consensus sequence, or lost when additional mutations were introduced into the CArG-box core (Fig. 2b, c). Another site with a perfect CArG-box core, but with three mismatches to the 16-bp AG consensus sequence, was found 100 bp downstream from the stop codon. No clear binding of AG to this site was observed *in vitro* (data not shown).

To evaluate whether the AG binding site detected in the 3′ region is necessary for the AG-dependent induction of *SPL*, translational fusions between *SPL* and the *GUS* reporter gene were made and transformed into wild-type plants. Overall, GUS expression patterns in plant transgenic lines containing the wild-type *SPL–GUS* reporter gene fusion recapitulated the endogenous *SPL* messenger RNA expression pattern[6] (Fig. 2d–h, see also Supplementary Fig. S3a–h). GUS expression started to appear at the lateral edges of the stamen primordia in stage 6 floral buds (Fig. 2e), and subsequently expanded, covering the developing stamens during stages 6–8 (Fig. 2f–h). In addition to the continued GUS expression in the developing stamens, staining was also observed in ovule primordia at stage 10, as well as in the nucellus, the integuments and the funiculus of developing ovules at stages 11–13 (see Supplementary Fig. S3a–g). In contrast, transgenic plants carrying a *SPL–GUS* fusion in which the putative AG-binding site had been mutated (leading to a loss of AG binding *in vitro*; see above), showed weaker overall GUS activity and reduced expression domains (Fig. 2i–l; see also Supplementary Fig. S3i–k). During stages 6–8, weak staining was observed at only the lateral sides of the stamen primordia, and not throughout the primordia as observed using the wild-type construct (Fig. 2i–l). In the ovules of the transgenic lines containing the mutated construct, staining was observed in the nucellus, and very weak staining was observed in the inner integuments; however, staining was not observed in the outer integuments or in the funiculus at stages 11–13 (compare Supplementary Fig. S3i–k with e–g). This loss of GUS staining in the integuments and the funiculus corresponds to the pattern of AG expression in developing ovules; AG is specifically expressed in the integuments and

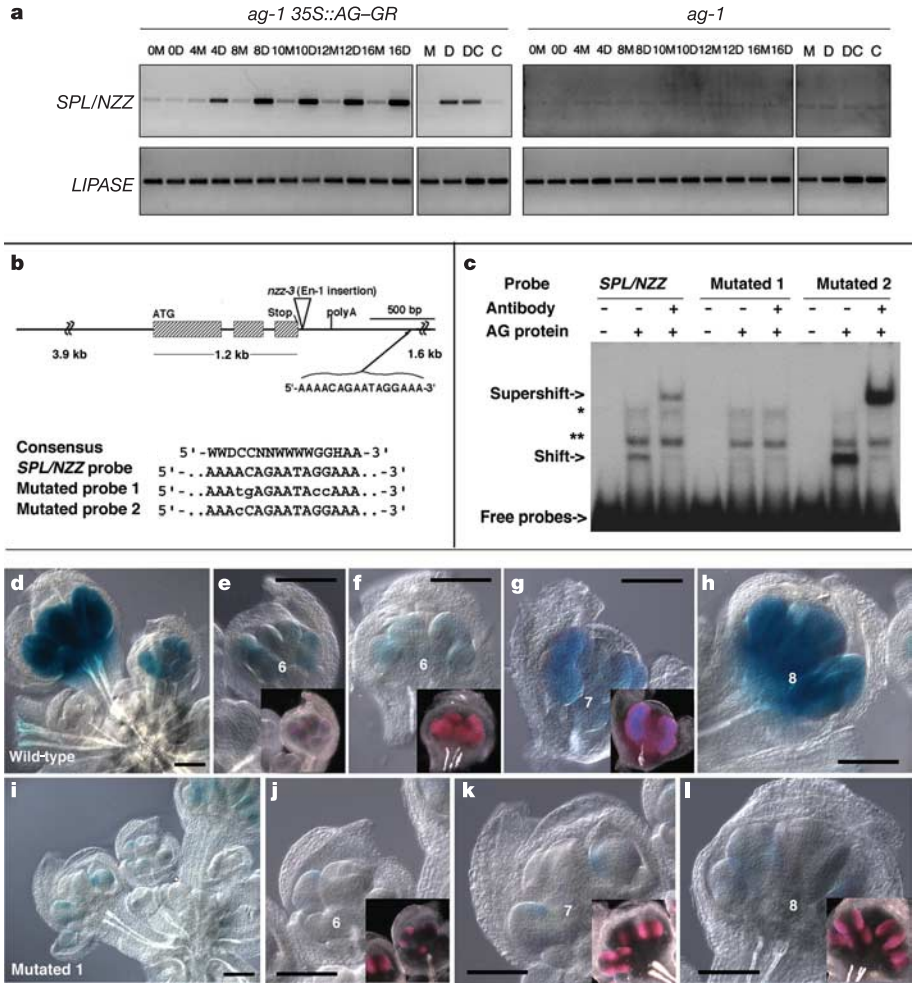

Figure 2 AG-mediated induction of *SPL* through a binding site in the 3′ region of the gene. **a**, RT–PCR for *SPL* (top) or for a ubiquitously expressed lipase gene (bottom) using RNA samples isolated from *ag-1 35S::AG–GR* plants (left) or control *ag-1* plants (right) 0, 4, 8, 10, 12 or 16 h after mock (M) or DEX (D) treatment. The smaller panels show the results for samples 4 h after simultaneous treatment with DEX and 10 μM cycloheximide (DC) or cycloheximide alone (C). **b**, Diagram of the *SPL* genomic region (top), and the 16-bp consensus binding sequence of AG (bottom). The CArG-box-like sequence found 897 bp downstream from the stop codon of the *SPL* gene, as well as the mutations that were introduced in it (indicated with small letters) are shown. D, not C; H, not G; N, A/T/G/C; W, A/T. **c**, Electrophoretic mobility shift assay using recombinant AG protein tagged with the c-Myc epitope, anti-c-Myc monoclonal antibody (9E10) and the 30-bp oligonucleotide probes described in **b**. Single and double asterisks indicate nonspecific binding from the bacterial extract. **d**–**l**, GUS expression patterns in transgenic lines carrying *SPL–GUS* fusion constructs either with the wild-type (**d**–**h**) or with a mutated (**i**–**l**) CArG-box-like sequence. The mutation was the same as for the mutated probe 1 shown in **b**. GUS staining for both constructs was performed under the same conditions. At least ten independent lines for each construct were analysed and representative images are shown. Insets in **e**–**g** and **j**–**l** are dark-field images showing enhanced staining of half-magnifications. Numbers indicate floral stages[30]. Scale bars, 100 μm.

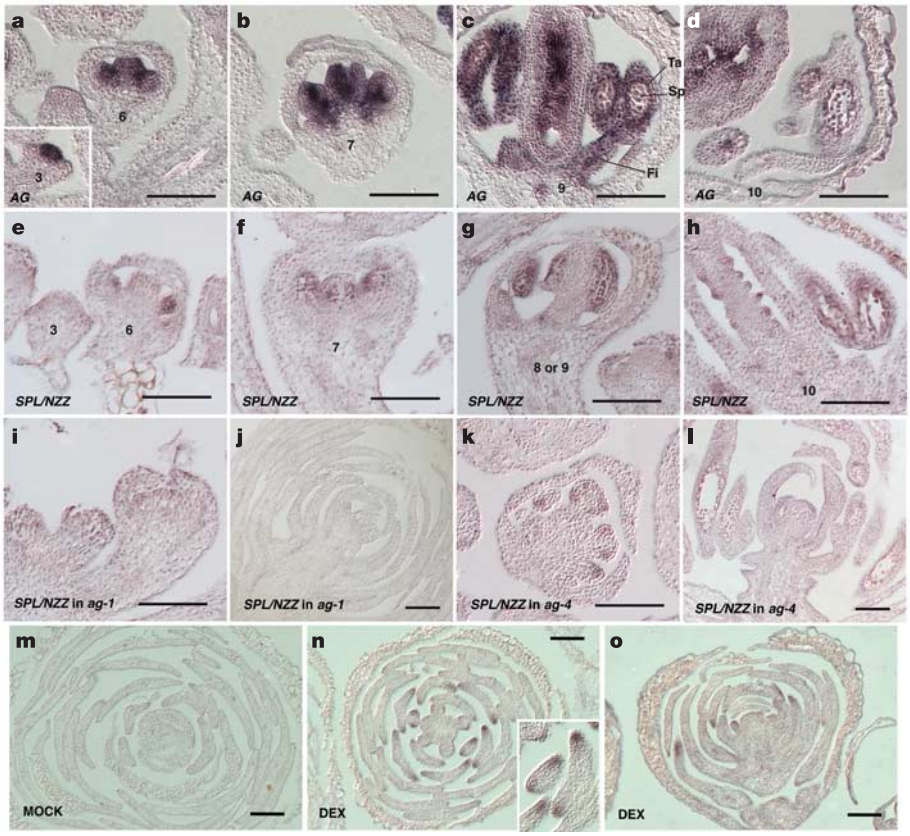

Figure 3 Expression of *SPL* and *AG* in wild-type flowers, and expression of *SPL* in flowers of *ag* mutants and in the lines with inducible AG activity. **a**–**h**, Expression of *AG* (**a**–**d**) and *SPL* (**e**–**h**) in wild-type flowers. **i**–**l**, Expression of *SPL* in *ag-1* (**i**, **j**) and *ag-4* (**k**, **l**) mutant flowers. **m**–**o**, *SPL* is induced by AG activity at the lateral edges of the distal part of organ primordia. Inflorescences of *ag-1 35S::AG–GR* plants were fixed 8 h after mock- (**m**) or DEX (**n**, **o**) treatment. Transverse (**m**, **n**) and longitudinal (**o**) sections were hybridized with a *SPL*-specific antisense probe. The inset in **n** shows the close-up view of the *SPL* signals. Numbers indicate floral stages[30]. Fi, filament; Sp, sporogenous cell; Ta, tapetum. Scale bars, 100 μm.

the funiculus of stage 11–12 flowers[5]. These results show that the CArG-box-like sequence in the 3′ region of the *SPL* gene, which is bound by AG *in vitro*, is necessary for normal *SPL* expression in developing stamens and ovules. The importance of the 3′ region of *SPL* for its function is further supported by the null *nzz-3* allele, which is caused by the insertion of a transposon 20-bp downstream from the stop codon[6] (Fig. 2b). Together, these data suggest that AG may bind to the 3′ region of the *SPL* gene and thus may directly regulate *SPL* expression during the development of the reproductive organs.

To determine whether AG is responsible for *SPL* expression throughout stamen development, the expression patterns of *SPL* and *AG* were compared in detail. The expression of *SPL* in stamen primordia during stages 6–7 was completely within the expression domain of *AG* (compare Fig. 3a, b with e, f). At stages 8–9, the *SPL* transcript was localized to tapetal and sporogenous cells (microspore mother cells)[6], whereas there was strong *AG* expression in the tapetum and the filament, but not in the sporogenous cells[3] (Fig. 3c, g). In anthers of stage 10 flowers, *SPL* expression continued in the tapetum and microspores[6], whereas *AG* was expressed in the tapetum, but not in microspores[3] (Fig. 3d, h). These partly overlapping expression patterns are in agreement with the idea that AG is required to activate *SPL* expression, but is not necessary for its maintenance. In the weak *ag-4* mutant, which produces flowers with stamens in whorl 3 (ref. 22), weak but distinct expression of *SPL* was observed in stamen primordia, but expression was barely detectable in sporogenous cells and inner organs of mature flowers (Fig. 3k, l). No clear expression of *SPL* was observed in the strong

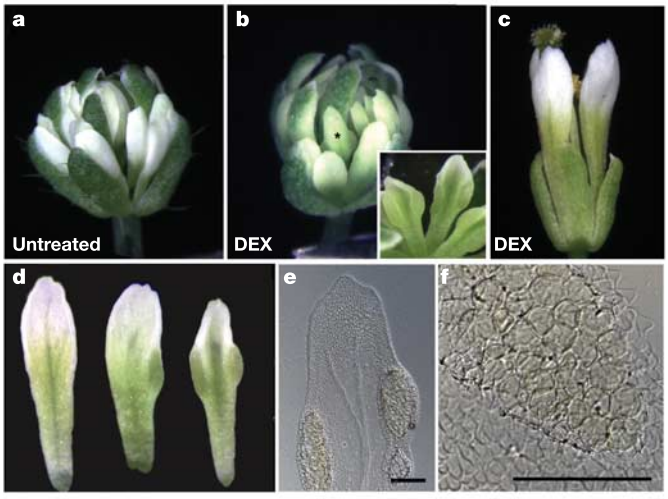

Figure 4 SPL is sufficient to induce microsporogenesis in the inner organs of *ag-1* mutant flowers. **a**, **b**, Flowers from *ag-1 35S::SPL–GR* transgenic plants untreated (**a**) or after continuous DEX treatment (**b**). The inset in **b** shows loculed petals produced in the inner whorls. DEX-treated non-transgenic *ag-1* plants did not show any loculed petals (data not shown). **c**, Flower from a *35S::SPL–GR* plant (wild-type background) after continuous DEX treatment. **d**, Normal-looking petal in whorl 2 (left) and loculed petals (middle and right) that developed in the inner whorls of a DEX-treated *ag-1 35S::SPL–GR* flower. **e**, **f**, Cleared view of loculed petals induced by ectopic SPL activity. Asterisk in **b** indicates an internal loculed petal. Scale bar, 100 μm.

ag-1 mutant allele (Fig. 3i, j), indicating that the induction of *SPL* expression is dependent on AG.

To obtain further evidence for the induction of *SPL* by AG, localization of *SPL* transcripts in flowers of *ag-1 35S::AG–GR* plants was examined. Eight hours after DEX treatment, induction of *SPL* was observed along the lateral edges of the distal parts of organ primordia, which matches the region where microsporogenesis is induced in stamenoid petals (compare Fig. 3m–o with Fig. 1d). This expression domain also coincides with the initial expression of *SPL* observed in the *SPL–GUS* reporter lines (Fig. 2e). No induction was observed in fully developed sepals or petals (Fig. 3n, o). These results demonstrate that AG specifically upregulates *SPL* expression in a developmentally controlled manner in specific floral tissues.

To test whether SPL can induce microsporogenesis in the absence of AG function, a *35S*::*SPL–GR* construct was used. The functionality of the SPL–GR fusion protein during microsporogenesis was confirmed in the *nzz-2* mutant background (data not shown). In transgenic lines in the *ag-1* background, loculed petals were observed after continuous DEX treatment (Fig. 4a, b). These loculed structures were similar to the ones induced by a single DEX treatment in *ag-1 35S*::*AG–GR* plants (compare Fig. 4b, e with Fig. 1d, e), and inside the locules, pollen grains were observed (Fig. 4f). This result shows that SPL can induce microsporogenesis in the absence of AG activity, suggesting that SPL acts as a central mediator for the function of AG in sporogenesis. Although SPL–GR was ectopically expressed, locule formation was observed in *ag-1* mutant flowers only at the lateral edges of organs in whorl 3 and inward; the ectopic locule formation was never observed in whorl 2 of DEX-treated flowers (Fig. 4c, d). These data suggest that other whorl-specific factors are involved in the induction of microsporogenesis.

Our results, together with the previous identification of *NAP* (an NAC-family transcription factor gene) as a late-stage target of APETALA3 (ref. 17), indicate that floral homeotic proteins control target genes with various functions throughout organ development. In addition, the interaction of AG and *SPL* shows the likelihood that AG activates other regulators that perform a subset of its functions. Therefore, this study provides direct evidence to support the idea that plant homeotic genes control organogenesis as part of a regulatory hierarchy. □

Methods

Plant materials and treatments

All plants used in this study were in the Landsberg *erecta* background, and were grown at 22 °C under constant illumination. Transgenic plants were generated by *Agrobacterium*-mediated infiltration. The *35S*::*AG–GR* construct was transformed into wild-type plants and the primary T1 transformants were screened by kanamycin selection. A line carrying a single transgene insertion, which showed the AG-overexpression phenotype[8] in a DEX-dependent fashion, was subsequently crossed into the *ag-1* background. The *35S*::*SPL–GR* construct was transformed directly into *ag-1*/+ plants, and the T1 plants were screened by Basta selection. Phenotypic analyses in the *ag-1* background were performed in the T1 generation, as well as in the T2 generation that was produced by selfing *ag-1*/+ T1 plants. One transgenic line for *35S*::*SPL–GR* was crossed to *nzz-2*/+ plants to obtain lines in the *nzz-2* mutant background in subsequent generations. The *SPL–GUS* constructs were transformed into wild-type plants. GUS staining was performed on the T1 plants screened by Basta selection. For continuous DEX treatment of the *ag-1 35S*::*AG–GR* or *ag-1 35S*::*SPL–GR* plants, the plants were watered with 10 μM DEX daily. For a single DEX treatment, the inflorescences were dipped in water containing 10 μM DEX and 0.015% Silwet L-77 (ref. 19). Cleared whole-mount observation was performed according to published protocols[23].

Plasmid constructs

The *35S*::*AG–GR* construct was produced as follows: the coding region of AG was amplified from inflorescence cDNA using primers P1 and P2 (see Supplementary Table 1) and cloned into a blunt-ended *Eco*RI site of pBluescript SK (Stratagene) to produce pSK–AG. To produce pSK–AG–GR, pSK–AG was digested with *Eco*RI, filled-in and ligated with a DNA fragment containing a rat glucocorticoid hormone binding domain[16], which was excised with *Bam*HI and *Xba*I from pRS020 (pDeltaGRBX)[17] and filled in. The *AG–GR* fragment was released from pSK–AG–GR by digestion with *Xba*I and *Cla*I, and ligated into the corresponding sites of the binary vector pMAT137 (a derivative of pMAT037; ref. 24) that contains tandem cauliflower mosaic virus 35S enhancers and a terminator. For the reporter gene constructs, a *SPL* 6,646-bp genomic fragment (positions 4,303–10,958 of BAC clone F27G19 (GenBank accession number AL078467)) comprising *SPL* and the flanking intergenic sequences was amplified using UltraPfu High-Fidelity DNA polymerase (Stratagene) with primers P3 and P4 (see Supplementary Table 1) and wild-type Columbia genomic DNA. The product was cloned into the pCR II vector (Invitrogen) to produce pCR–SPLG. pCR–SPLG was mutagenized in the 3′ CArG-box-like sequence (897-bp downstream from the stop codon) by using the Quikchange II XL site-directed mutagenesis kit (Stratagene) with primers P5 and P6 (see Supplementary Table 1) to produce pCR–SPLG-M3. Both pCR–SPLG and pCR–SPLG-M3 were digested with *Bsp*EI (6939 of F27G19), filled in and then ligated with a *Sfo*I-digested *GUS* fragment[25] to produce pCR–SPLG-ori–GUS and pCR–SPLG-M3–GUS, respectively. The *SPL–GUS* reporter fragments from pCR–SPLG-ori–GUS and pCR–SPLG-M3–GUS were cut out with *Asp*718 (later filled in) and *Not*I, and cloned into the binary vector pMlBart (a derivative of pART[26]) digested with *Ecl*136 and *Not*I. The *35S*::*SPL–GR* construct was produced as follows: *SPL* cDNA was amplified using primers P7 and P8 (see Supplementary Table 1), and cloned into the pCRII vector (Invitrogen) to produce pCR–SPL. To produce *35S*::*SPL–GR*, pCR–SPL was digested with *Mlu*I and *Xho*I, and the resulting insert was cloned into the pGreen0236TI vector, which is a derivative of pGreen0229 (ref. 27) containing a 35S promoter with tandem enhancers and the hormone binding domain of the rat glucocorticoid receptor followed by a 6 × haemagglutinin tag. The construction of the pG0236TI vector will be described elsewhere (T.I. and E.M.M., manuscript in preparation).

Microarray, RT–PCR and real-time PCR analysis

In the time course experiments after induction of AG activity, inflorescences containing floral buds of stages 1–10 were collected from *ag-1 35S*::*AG–GR* plants, the stems of which were about 5-cm long, 0, 4, 8, 10, 12 and 16 h after a single mock- or DEX treatment. Total RNA was isolated from tissue samples using Tri-reagent (Molecular Research Center Inc.) or the RNeasy Mini Kit (Qiagen). Two sets of independent RNA samples from *ag-1 35S*::*AG–GR* plants and two sets of RNA samples from the *ag-1* single mutant were prepared. Microarray experiments were performed as previously described[10,28]. For RT–PCR, total RNA was reverse-transcribed using the ThermoScript RT–PCR system (Invitrogen). As semi-quantitative RT–PCR, the expression of *SPL* (At4g27330) and a control lipase gene (At1g10740) were analysed using primers P9 and P10 after 30 cycles and primers P11 and P12 after 24 cycles, respectively (see Supplementary Table 1). The gel was blotted onto Hybond-N membrane and hybridized with ^{32}P-labelled *SPL* or lipase RT–PCR products. Real-time PCR was performed with the SYBR Green PCR Master Mix (Applied Biosystems) using the Applied Biosystems GeneAmp 5700 sequence detection system according to the manufacturer's instructions. The sequences of *SPL* primers P13 and P14 and actin control primers P15 and P16 used for real-time PCR are shown in Supplementary Table 1.

In vitro DNA binding assay

Electrophoretic mobility shift assays (EMSA) were performed as described[20]. Sequences of oligonucleotides for probes are shown in Supplementary Table 1. For the CArG-box-like sequence located 897-bp downstream from the stop codon (*SPL* probe; Fig. 2b, c), oligonucleotides O17 and O18 were used. Mutated versions of this probe were prepared with oligonucleotides O19 and O20 (mutated probe 1), and oligonucleotides O21 and O22 (mutated probe 2). For the site with a perfect CArG-box core located 100-bp downstream from the stop codon, oligonucleotides O23 and O24 were used. For supershift assays, a monoclonal anti-c-Myc antibody (9E10, Santa Cruz Biotechnology) was used[20].

In situ hybridization and GUS staining

Non-radioactive *in situ* hybridizations were performed as previously described[29]. To produce a *SPL*-specific anti-sense probe, the RT–PCR product was cloned into the pCRII vector (Invitrogen) and used as a template for *in vitro* transcription. The AG-specific probe was synthesized from plasmid pCIT565(*AG*)[4]. GUS staining was performed as previously described[25].

Received 9 May; accepted 7 June 2004; doi:10.1038/nature02733.

1. Bowman, J. L., Smyth, D. R. & Meyerowitz, E. M. Genes directing flower development in *Arabidopsis*. *Plant Cell* **1,** 37–52 (1989).
2. Yanofsky, M. F. *et al.* The protein encoded by the *Arabidopsis* homeotic gene *agamous* resembles transcription factors. *Nature* **346,** 35–39 (1990).
3. Bowman, J. L., Drews, G. N. & Meyerowitz, E. M. Expression of the *Arabidopsis* floral homeotic gene *AGAMOUS* is restricted to specific cell types late in flower development. *Plant Cell* **3,** 749–758 (1991).
4. Drews, G. N., Bowman, J. L. & Meyerowitz, E. M. Negative regulation of the *Arabidopsis* homeotic gene *AGAMOUS* by the *APETALA2* product. *Cell* **65,** 991–1002 (1991).
5. Reiser, L. *et al.* The *BELL1* gene encodes a homeodomain protein involved in pattern formation in the *Arabidopsis* ovule primordium. *Cell* **83,** 735–742 (1995).
6. Schiefthaler, U. *et al.* Molecular analysis of *NOZZLE*, a gene involved in pattern formation and early sporogenesis during sex organ development in *Arabidopsis thaliana*. *Proc. Natl Acad. Sci. USA* **96,** 11664–11669 (1999).
7. Yang, W. C., Ye, D., Xu, J. & Sundaresan, V. The *SPOROCYTELESS* gene of *Arabidopsis* is required for initiation of sporogenesis and encodes a novel nuclear protein. *Genes Dev.* **13,** 2108–2117 (1999).
8. Mizukami, Y. & Ma, H. Ectopic expression of the floral homeotic gene *AGAMOUS* in transgenic *Arabidopsis* plants alters floral organ identity. *Cell* **71,** 119–131 (1992).
9. Honma, T. & Goto, K. Complexes of MADS-box proteins are sufficient to convert leaves into floral organs. *Nature* **409,** 525–529 (2001).
10. Wellmer, F., Riechmann, J. L., Alves-Ferreira, M. & Meyerowitz, E. M. Genome-wide analysis of spatial gene expression in *Arabidopsis* flowers. *Plant Cell* **16,** 1314–1326 (2004).
11. Gustafson-Brown, C., Savidge, B. & Yanofsky, M. F. Regulation of the *Arabidopsis* floral homeotic gene *APETALA1*. *Cell* **76,** 131–143 (1994).

12. Savidge, B., Rounsley, S. D. & Yanofsky, M. F. Temporal relationship between the transcription of two *Arabidopsis* MADS box genes and the floral organ identity genes. *Plant Cell* **7,** 721–733 (1995).
13. Lenhard, M., Bohnert, A., Jurgens, G. & Laux, T. Termination of stem cell maintenance in *Arabidopsis* floral meristems by interactions between *WUSCHEL* and *AGAMOUS*. *Cell* **105,** 805–814 (2001).
14. Liljegren, S. J. *et al. SHATTERPROOF* MADS-box genes control seed dispersal in *Arabidopsis*. *Nature* **404,** 766–770 (2000).
15. Pinyopich, A. *et al.* Assessing the redundancy of MADS-box genes during carpel and ovule development. *Nature* **424,** 85–88 (2003).
16. Lloyd, A. M., Schena, M., Walbot, V. & Davis, R. W. Epidermal cell fate determination in *Arabidopsis*: patterns defined by a steroid-inducible regulator. *Science* **266,** 436–439 (1994).
17. Sablowski, R. W. & Meyerowitz, E. M. A homolog of *NO APICAL MERISTEM* is an immediate target of the floral homeotic genes *APETALA3/PISTILLATA*. *Cell* **92,** 93–103 (1998).
18. Balasubramanian, S. & Schneitz, K. *NOZZLE* links proximal-distal and adaxial-abaxial pattern formation during ovule development in *Arabidopsis thaliana*. *Development* **129,** 4291–4300 (2002).
19. Wagner, D., Sablowski, R. W. & Meyerowitz, E. M. Transcriptional activation of *APETALA1* by LEAFY. *Science* **285,** 582–584 (1999).
20. Shiraishi, H., Okada, K. & Shimura, Y. Nucleotide sequences recognized by the AGAMOUS MADS domain of *Arabidopsis thaliana in vitro*. *Plant J.* **4,** 385–398 (1993).
21. Huang, H., Mizukami, Y., Hu, Y. & Ma, H. Isolation and characterization of the binding sequences for the product of the *Arabidopsis* floral homeotic gene *AGAMOUS*. *Nucleic Acids Res.* **21,** 4769–4776 (1993).
22. Sieburth, L. E., Running, M. P. & Meyerowitz, E. M. Genetic separation of third and fourth whorl functions of *AGAMOUS*. *Plant Cell* **7,** 1249–1258 (1995).
23. Schneitz, K., Hülskamp, M. & Pruitt, R. E. Wild-type ovule development in *Arabidopsis thaliana*: a light microscope study of cleared whole-mount tissue. *Plant J.* **7,** 731–749 (1995).
24. Matsuoka, K. & Nakamura, K. Propeptide of a precursor to a plant vacuolar protein required for vacuolar targeting. *Proc. Natl Acad. Sci. USA* **88,** 834–838 (1991).
25. Ito, T., Sakai, H. & Meyerowitz, E. M. Whorl-specific expression of the *SUPERMAN* gene of *Arabidopsis* is mediated by *cis* elements in the transcribed region. *Curr. Biol.* **13,** 1524–1530 (2003).
26. Gleave, A. P. A versatile binary vector system with a T-DNA organisational structure conducive to efficient integration of cloned DNA into the plant genome. *Plant Mol. Biol.* **20,** 1203–1207 (1992).
27. Hellens, R. P., Edwards, E. A., Leyland, N. R., Bean, S. & Mullineaux, P. M. pGreen: a versatile and flexible binary Ti vector for *Agrobacterium*-mediated plant transformation. *Plant Mol. Biol.* **42,** 819–832 (2000).
28. Wagner, D. *et al.* Floral induction in tissue culture: a system for the analysis of LEAFY-dependent gene regulation. *Plant J.* **39,** 273–282 (2004).
29. Long, J. A. & Barton, M. K. The development of apical embryonic pattern in *Arabidopsis*. *Development* **125,** 3027–3035 (1998).
30. Smyth, D. R., Bowman, J. L. & Meyerowitz, E. M. Early flower development in *Arabidopsis*. *Plant Cell* **2,** 755–767 (1990).

Supplementary Information accompanies the paper on **www.nature.com/nature**.

Acknowledgements We thank J. Chow for experimental help; M. Hasebe; former Meyerowitz laboratory members, J. A. Long, K. Goto, M. Frohlich and P. Kumar; and current laboratory members, especially P. Sieber, I. Negrutiu, A. Dubois, C. Ohno, C. Baker, E. Haswell, M. Heisler, V. R. Gonehal and Y. X. Zhao for comments on the manuscript. M.A-F. is indebted to IPBO and M. Van Montagu for a fellowship sponsored by Aventis CropSciences. This work was supported by a grant from the National Institutes of Health to E.M.M.

Competing interests statement The authors declare that they have no competing financial interests.

Correspondence and requests for materials should be addressed to E.M.M. (meyerow@its.caltech.edu).

First cleavage plane of the mouse egg is not predetermined but defined by the topology of the two apposing pronuclei

Takashi Hiiragi & Davor Solter

Max-Planck Institute of Immunobiology, D-79108 Freiburg, Germany

Studies of experimentally manipulated embryos[1–4] have led to the long-held conclusion that the polarity of the mouse embryo remains undetermined until the blastocyst stage. However, recent studies[5–7] reporting that the embryonic–abembryonic axis of the blastocyst arises perpendicular to the first cleavage plane, and hence to the animal–vegetal axis of the zygote, have led to the claim that the axis of the mouse embryo is already specified in the egg. Here we show that there is no specification of the axis in the egg. Time-lapse recordings show that the second polar body does not mark a stationary animal pole, but instead, in half of the embryos, moves towards a first cleavage plane. The first cleavage plane coincides with the plane defined by the two apposing pronuclei once they have moved to the centre of the egg. Pronuclear transfer experiments confirm that the first cleavage plane is not determined in early interphase but rather is specified by the newly formed topology of the two pronuclei. The microtubule networks that allow mixing of parental chromosomes before dividing into two may be involved in these processes.

Polarity formation of the mammalian preimplantation embryo remains a controversial subject. Because of their highly regulative capacity in coping with experimental manipulations (for example, blastomere isolation[1–3] and chimaera formation[4]) mouse embryos have long been thought to lack polarity until the blastocyst stage. Recently this assumption has been challenged in two independent approaches[6,7] showing that the embryonic–abembryonic (Em–Ab) axis of the mouse blastocyst is perpendicular to the first cleavage plane. Considering the second polar body (2pb) as a stationary marker of the animal pole during preimplantation development, the authors concluded that polarity of the mouse embryo is specified in the egg, as it is for most non-mammalian animals. Possible movement of the 2pb was dismissed as 'occasional'[5,6]. It has also been proposed that the plane of initial cleavage passes through both the sperm entry position (SEP) and the 2pb, and that the SEP can define the future Em–Ab axis of the embryo[8,9]. However, our preliminary

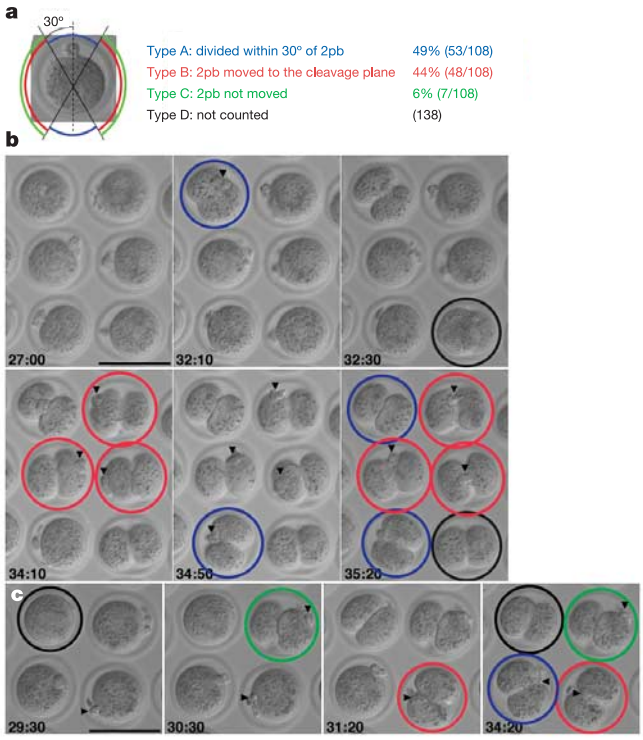

Figure 1 The 2pb moves towards the first cleavage plane in half the embryos. **a**, Embryos are classified into four types: type A (blue), divided within 30° of the 2pb; type B (red), the 2pb moved towards the first cleavage plane; type C (green), the 2pb did not reach the cleavage plane; type D (black), not counted due to the unclear topological relationship. **b**, **c**, Sequential DIC images of embryos cultured *in vitro*. The embryos assigned to each type are marked with coloured circles. Arrowheads indicate the 2pb. In each frame, time is given in h:min after hCG injection. Scale bars represent 100 μm.